Thermally activated intersubband scattering and oscillating magnetoresistance in quantum wells

S. Wiedmann,[1,2] G. M. Gusev,[3] O. E. Raichev,[4] A. K. Bakarov,[5] and J. C. Portal[1,2,6]

[1]*LNCMI, UPR 3228, CNRS-INSA-UJF-UPS, BP 166, 38042 Grenoble Cedex 9, France*
[2]*INSA Toulouse, 31077 Toulouse Cedex 4, France*
[3]*Instituto de Física, Universidade de São Paulo, CP 66318, CEP 05315-970 São Paulo, SP, Brazil*
[4]*Institute of Semiconductor Physics, NAS of Ukraine, Prospekt Nauki 41, 03028 Kiev, Ukraine*
[5]*Institute of Semiconductor Physics, Novosibirsk 630090, Russia*
[6]*Institut Universitaire de France, 75005 Paris, France*

Experimental studies of magnetoresistance in high-mobility wide quantum wells reveal oscillations which appear with an increase in temperature to 10 K and whose period is close to that of Shubnikov-de Haas oscillations. The observed phenomenon is identified as magnetointersubband oscillations caused by the scattering of electrons between two occupied subbands and the third subband which becomes occupied as a result of thermal activation. These small-period oscillations are less sensitive to thermal suppression than the large-period magnetointersubband oscillations caused by the scattering between the first and the second subbands. Theoretical study, based on consideration of electron scattering near the edge of the third subband, gives a reasonable explanation of our experimental findings.

I. INTRODUCTION

Magnetoresistance oscillations caused by Landau quantization provide important information about fundamental properties of electron system in solids. Studies of the Shubnikov-de Haas (SdH) oscillations due to sequential passage of Landau levels through the Fermi level[1] allow one to investigate the shape of the Fermi surface as well as the scattering processes leading to Landau-level broadening. Apart from SdH oscillations, there exist oscillating phenomena which are not related to the position of Landau levels with respect to the Fermi level and, therefore, are less sensitive to temperature. One of the most important examples of such phenomena are the magnetointersubband (MIS) oscillations[2] observed in two-dimensional (2D) electron systems with two or more populated dimensional-quantization subbands, which are realized in single, double, and triple quantum wells.[3–10] Recently, magneto-oscillations driven by intersubband transitions have also been reported for 2D electrons on liquid helium.[11] The peculiar magnetoresistance properties of 2D electron systems are caused by the possibility of elastic (impurity-assisted) scattering of electrons between the subbands. The MIS oscillations occur because of a periodic modulation of the probability of intersubband transitions by the magnetic field. The maxima of these oscillations correspond to the condition when subband splitting energy Δ is a multiple of the cyclotron energy $\hbar\omega_c$, so the Landau levels belonging to different subbands are aligned. Since MIS oscillations survive an increase in temperature, they are used to study electron-scattering mechanisms at elevated temperatures when SdH oscillations completely disappear in the region of weak magnetic fields.[6,8–10]

Despite the fact that MIS oscillations are one of the most fundamental manifestations of quantum magnetotransport, their properties are not sufficiently studied. In particular, the case when one of the subbands is placed close to the Fermi energy and its filling by electrons is very small deserves a closer attention. Theoretical studies[12] confirmed that MIS oscillations can exist at such small fillings of the upper subband but a detailed experimental investigation of this interesting situation is still missing. From the theoretical point of view, it is important to consider scattering mechanisms of electrons near the edge of the weakly populated subband and a possibility of probing these mechanisms by magnetoresistance measurements.

We have studied magnetoresistance in symmetric GaAs wide quantum wells (WQWs) with high-mobility 2D electron gas. Owing to a high electron density and a large well width, these systems form a bilayer configuration due to charge redistribution, when two quantum wells near the interfaces are separated by an electrostatic potential barrier (see Fig. 1). The presence of the two occupied subbands is confirmed by the observation of MIS oscillations in magnetoresistance. Apart from MIS and SdH oscillations, we ob-
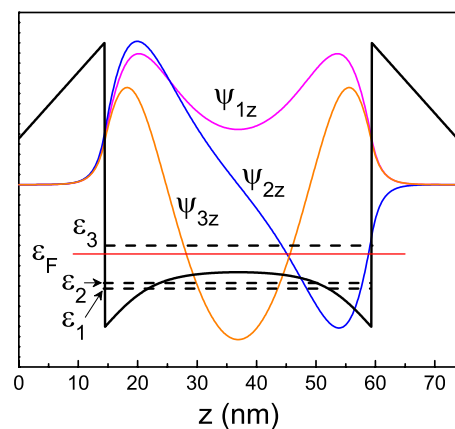

FIG. 1. (Color online) Calculated confinement potential profile of our wide quantum wells and wave functions of electrons for the first three subbands. Positions of the subbands (straight dashed lines) and the Fermi level (straight solid line) are schematically shown.

serve unusual oscillations which appear when temperature is raised to 10 K and persist up to $T=40$ K in the region of magnetic fields from 0.35 to 2 T. The period of these oscillations is slightly smaller than the period of SdH oscillations. The dependence of resistivity on magnetic field and temperature allows us to treat these small-period oscillations as the MIS oscillations caused by electron scattering between the two lowest subbands and the third subband which is placed slightly above the Fermi energy ε_F (Fig. 1) and becomes populated as a result of thermal activation. This conclusion is supported by a theoretical consideration of magnetoresistance, which also uncovers the scattering mechanism responsible for Landau-level broadening and thereby explains the unusual low sensitivity of the small-period MIS oscillations to thermal suppression at elevated temperatures. The calculated magnetoresistance is in good agreement with the experimental results.

The paper is organized as follows. Section II presents experimental details and results. Section III gives theoretical calculation of magnetoresistance and its application to analysis and discussion of the experimental data. Concluding remarks are given in the last section. The Appendix is devoted to calculation of quantum lifetime of electrons in the upper subband.

II. MAGNETORESISTANCE MEASUREMENTS

We have studied wide GaAs quantum wells ($w=45$ nm) with an electron density of $n_s \simeq 9.2 \times 10^{11}$ cm^{-2} and a mobility of $\mu \simeq 1.9 \times 10^6$ cm^2/V s at low temperatures. To achieve both high density and high mobility, the samples have been produced according to Ref. 13, where the barriers surrounding the quantum well are formed by short-period AlAs/GaAs superlattices. Samples in both Hall bar ($l \times w = 250~\mu m \times 50~\mu m$) and van der Pauw (size 3 mm $\times 3$ mm) geometries have been studied. The two lowest subbands are separated by the energy $\Delta_{12}=1.40$ meV, extracted from MIS oscillation periodicity.[6] This value is in agreement with a self-consistent numerical calculation of the electron energy spectrum and wave functions (Fig. 1). The small energy separation and the symmetry of the wave functions for the two lowest subbands show that the corresponding (symmetric and antisymmetric) states are formed as a result of tunnel hybridization of the states in two quantum wells near the interfaces. Measurements of the longitudinal resistance R_{xx} have been carried out in a perpendicular magnetic field B up to 2.5 T in a cryostat with a variable-temperature insert in the temperature range from 1.4 to 40 K. As confirmed by theoretical estimates, see Eq. (8) and Fig. 6 below, the magnetoresistance measurements in the fields below 0.5 T are performed in the regime of overlapping Landau levels.

The main results for the magnetoresistance are summarized in Fig. 2. Several groups of quantum oscillations, periodic with the inverse magnetic field, are observed. At low temperatures we see both SdH (small-period) and MIS (large-period) oscillations, the latter are caused by electron scattering between the two lowest subbands. SdH oscillations are visible at 4.2 K in the region of magnetic fields above 0.6 T. In this region, SdH oscillations are superim-
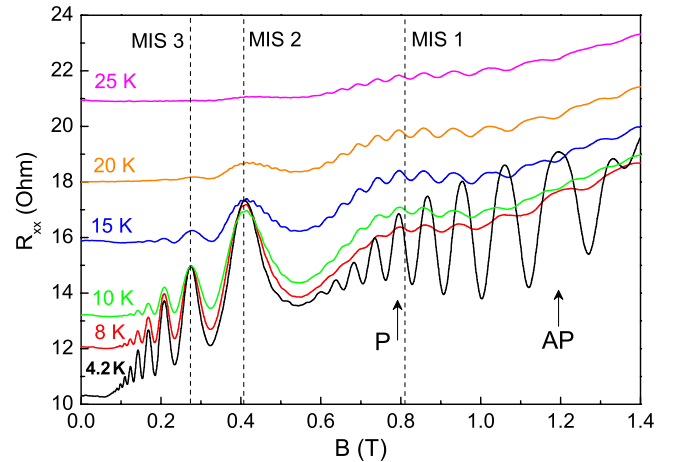

FIG. 2. (Color online) (a) Measured longitudinal resistance of a two-subband system at different temperatures from 4.2 to 25 K. The vertical dashed lines indicate positions of the three main MIS peaks. As temperature increases, the SdH oscillations are replaced by a new kind of oscillations which have a smaller period and survive at high temperatures. We identify these oscillations as MIS oscillations associated with the third subband.

posed on the first MIS peak whose maximum is placed at $B \simeq 0.8$ T corresponding to the alignment condition $\hbar\omega_c = \Delta_{12}$. With increasing temperature, the SdH oscillations are rapidly damped and disappear. Disappearance of SdH oscillations for $T > 4.2$ K and in the range of magnetic fields studied in the present work can be easily confirmed applying the well-known Lifshitz-Kosevich formula containing the specific thermal damping factor $(2\pi^2 T/\hbar\omega_c)/\sinh(2\pi^2 T/\hbar\omega_c)$. However, another oscillating pattern is developed at $T \sim 10$ K and persists even at $T > 25$ K, when large-period MIS oscillations are strongly damped. The period of these high-temperature oscillations is close to the SdH oscillation period but does not coincide with it. For example, the SdH peak at $B \simeq 0.8$ T appears to be in phase with the high-temperature oscillations (arrow P in Fig. 2) while the SdH peak at $B \simeq 1.2$ T stays in antiphase (arrow AP in Fig. 2). At $B \sim 1$ T, the high-temperature oscillations replace SdH oscillations in the interval from $T=8$ to 10 K. As seen from the plots for 10, 15, and 20 K, the high-temperature oscillations also exist in the region of lower magnetic fields corresponding to the second MIS peak.

Therefore, the nature of the small-period high-temperature oscillations is obviously different from the nature of SdH oscillations. The origin of these oscillations can be understood if the third subband in our quantum well is included into consideration. Indeed, numerical calculations of WQW energy spectrum show that at $T=0$ the third subband should be weakly populated at the given electron density. The fact that we do not observe the effects associated with the third subband at low temperatures indicates a possible error within a few meV in theoretical determination of the position of this subband. If we assume that the third subband is placed slightly above the Fermi energy ($\varepsilon_3 > \varepsilon_F$) and attribute the small-period oscillations to MIS oscillations owing to electron transitions between this subband and the subbands 1 and 2, the observed properties of these oscilla-
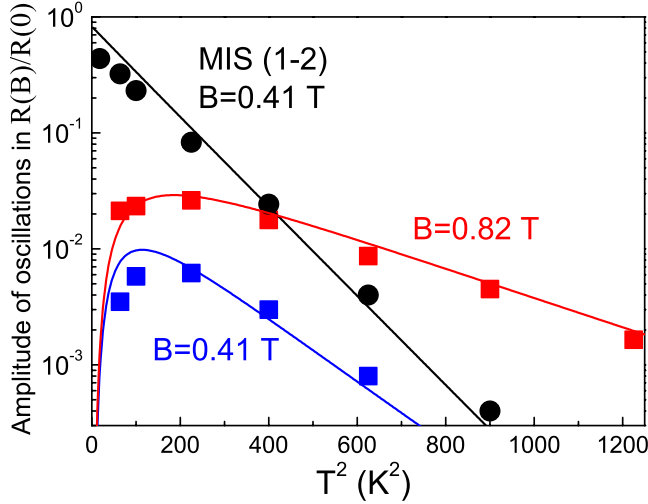
FIG. 3. (Color online) Temperature dependence of the amplitudes of small-period (squares) and large-period (circles) MIS oscillations. The solid lines are the results of theoretical calculation (see Sec. III for details).

tions become clear. First, the periodicity in this case is determined by the large splitting energies $\Delta_{13} = \varepsilon_3 - \varepsilon_1$ and $\Delta_{23} = \varepsilon_3 - \varepsilon_2$, which also explains a slightly smaller period of these oscillations compared to SdH oscillations. Next, the thermal activation behavior is explained by the increasing number of electrons being able to participate in the intersubband transitions with increasing temperature. Finally, the persistence of the oscillations at high temperatures follows from their nature: a suppression of MIS oscillations with temperature is not related to thermal smearing of the Fermi surface but is caused by thermal broadening of Landau levels.

The problem of temperature behavior deserves a more detailed discussion. Figure 3 shows temperature dependence of the amplitudes (peak-to-peak values) for the small-period MIS oscillations superimposed on the maxima of the first and second large-period MIS peaks, $B = 0.82$ and 0.41 T. For comparison, a similar dependence for the amplitude of the second MIS peak is shown. The plots demonstrate a notable difference in behavior for these two kinds of MIS oscillations. While large-period MIS oscillations are monotonically suppressed by temperature, the small-period oscillations are characterized by a nonmonotonic dependence with a maximum around 10–15 K and a slower decrease with temperature. In the region of high temperatures, all the experimental plots apparently show that the logarithm of the amplitude linearly decreases with T^2. The slope of this decrease linearly scales with B^{-1}, as can be seen by comparison of the small-period MIS oscillation amplitudes at 0.41 and 0.82 T. These data suggest that the suppression of both small-period and large-period MIS oscillations is governed by the same mechanism, thermal broadening of Landau levels due to enhancement of electron-electron scattering with temperature. Such an effect is described in terms of temperature-dependent quantum lifetime of electrons, $\tau(T)$, entering the Dingle factor d, the latter determines the oscillation amplitude

$$d = \exp[-\pi/\omega_c \tau(T)],$$

$$\frac{1}{\tau(T)} = \frac{1}{\tau(0)} + \frac{1}{\tau^{ee}(T)}, \quad \frac{1}{\tau^{ee}(T)} = \lambda \frac{T^2}{\hbar \varepsilon_F}, \quad (1)$$

where $\tau(0)$ is the quantum lifetime due to elastic scattering. The term $1/\tau^{ee}$, where λ is a numerical constant on the order of unity, describes the partial contribution of electron-electron scattering, which in high-mobility samples dominates starting from $T \simeq 10$–15 K. The reliability of Eq. (1) has been proved in numerous magnetoresistance experiments; see Refs. 6, 8, 10, and 14 and references therein, and constant λ has been calculated for similar experimental conditions, see Refs. 15 and 16. It is also worth noting that the Dingle factor in Eq. (1) can be different for MIS and SdH oscillation amplitudes. First, owing to the specific energy dependence of the electron-electron scattering time, the electron-electron interaction does not suppress SdH oscillations.[17–19] Next, MIS oscillations are not sensitive to inhomogeneity of the electron density in contrast to SdH oscillations.[20,21] In our experiment, the quantum lifetime is extracted from MIS oscillations since SdH oscillations are already damped in the temperature interval under consideration.

However, by comparing the slopes of high-temperature suppression of small-period and large-period MIS oscillation amplitudes in Fig. 3 at the same magnetic field (0.41 T), it is evident that the small-period oscillations are more robust with respect to increasing temperature. This interesting and unexpected result may indicate a weaker temperature dependence of the Landau-level broadening in the third subband compared to subbands 1 and 2. Such an assumption is confirmed by theoretical calculations. The theoretical analysis carried out in the next section demonstrates that the consideration of electron scattering near the edge of the third subband explains the whole set of the data obtained in our magnetoresistance measurements.

III. THEORETICAL STUDY

In the experimentally relevant range of transverse magnetic fields, when the number of Landau levels below the Fermi energy is large, the electron transport in 2D systems is conveniently described by using either a quantum Boltzmann equation or Kubo formalism based on treatment of electron scattering within the self-consistent Born approximation.[22,23] These methods are straightforwardly generalized for many-subband systems.[10,24,25] By considering the elastic scattering of electrons in the limit of classically strong magnetic fields (when ω_c is much larger than transport scattering rates), one can express the linear dissipative resistivity of the electron system with several occupied 2D subbands in the following way:[24]

$$\rho_d = \frac{m}{e^2 n_s^2} \sum_{jj'} \int d\varepsilon \left(-\frac{\partial f_\varepsilon}{\partial \varepsilon} \right) \frac{k_{j\varepsilon}^2 + k_{j'\varepsilon}^2}{4\pi} \nu_{jj'}^{tr}(\varepsilon) D_{j\varepsilon} D_{j'\varepsilon}, \quad (2)$$

where m is the effective electron mass, e is the electron charge, j is the subband index, $k_{j\varepsilon} = \sqrt{2m(\varepsilon - \varepsilon_j)}/\hbar$ is the elec-

tron wave number in the subband j, ε_j is the subband energy, f_ε is the equilibrium (Fermi-Dirac) distribution function of electrons, and $D_{j\varepsilon}$ is the dimensionless (normalized to its zero-field value $m/\pi\hbar^2$) density of electron states in the subband j. The quantity $\nu_{jj'}^{tr}(\varepsilon)$ is defined as

$$\nu_{jj'}^{tr}(\varepsilon) = \frac{m}{\hbar^3} \int_0^{2\pi} \frac{d\theta}{2\pi} w_{jj'}[q_{jj'}(\varepsilon)] \frac{q_{jj'}^2(\varepsilon)}{k_{j\varepsilon}^2 + k_{j'\varepsilon}^2},$$

$$q_{jj'}^2(\varepsilon) = k_{j\varepsilon}^2 + k_{j'\varepsilon}^2 - 2k_{j\varepsilon}k_{j'\varepsilon}\cos\theta, \quad (3)$$

where $w_{jj'}(q)$ is the spatial Fourier transform of the correlators of random scattering potential, $q_{jj'}(\varepsilon)$ is the wave number transferred in elastic collisions, and θ is the scattering angle. In many cases, energy dependence of k_j and $w_{jj'}(q)$ can be neglected within the interval of thermal smearing of the electron distribution. Then $k_{j\varepsilon}$ are taken at the Fermi surface, $k_{j\varepsilon} = k_{j\varepsilon_F} = \sqrt{2\pi n_j}$, where n_j is the sheet electron density in the subband j and $\nu_{jj'}^{tr}(\varepsilon)$ are reduced to transport scattering rates $\nu_{jj'}^{tr}$ defined, for example, in Ref. 26.

In our samples, where two lowest subbands are closely spaced and almost equally populated while the third subband is weakly populated, we have $k_1^2 \simeq k_2^2 \gg k_3^2$. Application of Eq. (2) under these conditions gives us the following expression:

$$\rho_d = \frac{m}{2e^2 n_s} \int d\varepsilon \left(-\frac{\partial f_\varepsilon}{\partial \varepsilon}\right) [\nu_{11}^{tr} D_{1\varepsilon}^2 + \nu_{22}^{tr} D_{2\varepsilon}^2 + 2\nu_{12}^{tr} D_{1\varepsilon} D_{2\varepsilon}$$
$$+ (\nu_{13}^{tr} D_{1\varepsilon} + \nu_{23}^{tr} D_{2\varepsilon}) D_{3\varepsilon}]. \quad (4)$$

The scattering potential in our samples is created mostly by donor impurities localized in the side barrier regions, so the correlation between the effective scattering potentials in the layers of the double-layer system formed in our WQWs can be neglected. Under this condition, see Ref. 24, the scattering in a symmetric double-layer system is described by equal correlators $w_{11}(q) = w_{22}(q) = w_{12}(q)$. Although this equality is based on a tight-binding description of the double-layer system it holds with good accuracy in our WQWs, as confirmed by calculations of the wave functions for the first and second subbands. Thus, in the case of closely spaced first and second subbands ($k_1 \simeq k_2$), the intrasubband and intersubband rates are almost equal, so we use $\nu_{11}^{tr} = \nu_{22}^{tr} = \nu_{12}^{tr} \equiv \nu_{tr}/2$. For the same reasons, the scattering rates between the lower subbands and the upper (third) subband are almost independent of the lower subband number. Indeed, since $k_{3\varepsilon} \simeq 0$, one has $\nu_{13}^{tr} = m w_{13}(k_1)/\hbar^3$ and $\nu_{23}^{tr} = m w_{23}(k_2)/\hbar^3$ with $k_1 \simeq k_2$ while the symmetry of the wave functions and the absence of interlayer correlations cause $w_{13}(q) \simeq w_{23}(q)$. Therefore, under the approximations valid for our samples Eq. (2) is finally rewritten as

$$\rho_d = \frac{m\nu_{tr}}{e^2 n_s} \int d\varepsilon \left(-\frac{\partial f_\varepsilon}{\partial \varepsilon}\right) [D_\varepsilon^2 + \eta D_\varepsilon D_{3\varepsilon}], \quad (5)$$

where $D_\varepsilon = (D_{1\varepsilon} + D_{2\varepsilon})/2$ and $\eta = \nu_{13}^{tr}/\nu_{tr} = \nu_{23}^{tr}/\nu_{tr}$. Notice that the dimensionless parameter η is expected to be considerably smaller than unity because of a strong suppression of the correlators $w_{jj'}(q)$ at large q in the case of scattering by a smooth potential created by remote impurities.

The first term in Eq. (5), proportional to D_ε^2, describes positive magnetoresistance with MIS oscillations, typical for double-layer systems.[6,27] The second term is a correction due to elastic scattering of electrons between the lower subbands and the third subband. This correction is essentially determined by the density of states in the third subband, $D_{3\varepsilon}$, which experience a broadened steplike growth from zero at the edge of this subband, $\varepsilon = \varepsilon_3$. Since in our case $\varepsilon_3 > \varepsilon_F$, the third-subband contribution is not essential at low temperatures, when $-\partial f_\varepsilon/\partial \varepsilon$ is negligible at $\varepsilon > \varepsilon_3$. However, when temperature increases and the third subband becomes occupied, thermal activation of the elastic scattering between this subband and the two lower ones occurs. The second term in Eq. (5) then plays an important role, leading to small-period MIS oscillations which we observe in our experiment. As specified above, the magnitude of the parameter η, which determines the difference in the amplitudes between the two kinds of MIS oscillations, is affected by the spatial scale of the scattering potential.

To describe the small-period MIS oscillations, it is crucial to consider the density of states in the third subband by focusing on the scattering mechanisms which are responsible for its broadening and temperature dependence. The density of states $D_{j\varepsilon}$ for subband j can be found from the general expression

$$D_{j\varepsilon} = \frac{\hbar\omega_c}{\pi} \sum_{n=0}^{\infty} \text{Im}\, G_{\varepsilon jn}^A,$$

$$G_{\varepsilon jn}^A = \frac{1}{\varepsilon - \varepsilon_j - \hbar\omega_c(n+1/2) - \Sigma_{\varepsilon jn}^A}, \quad (6)$$

where $G_{\varepsilon jn}^A$ is the advanced (index A) Green's function for the electron in subband j in the Landau-level representation and $\Sigma_{\varepsilon jn}^A$ is the corresponding self-energy. The problem of determination of $\Sigma_{\varepsilon jn}^A$ in the general case is complicated and does not have an exact solution near the subband edge. Nevertheless, a physically reasonable result for $j=3$ can be obtained under a simplifying approach, when $\Sigma_{\varepsilon 3n}^A$ is replaced by $i\hbar/2\tau_3$, where τ_3 is the quantum lifetime in the subband 3 calculated in the free-electron approximation. In clean samples like ours, the main scattering mechanism contributing to the self-energy in the important temperature region $T \gtrsim 10$ K is the electron-electron scattering, so we estimate τ_3 based on this scattering mechanism, $\tau_3 \simeq \tau_3^{ee}$. The corresponding calculation is done in the Appendix and leads to the result

$$\frac{\hbar}{\tau_3^{ee}} = \kappa_0(T) \frac{T^{3/2}}{\sqrt{\varepsilon_F}}, \quad (7)$$

where $\kappa_0(T)$ is a dimensionless function of temperature which depends on the form of the wave functions ψ_{jz} shown in Fig. 1. This function is presented in Fig. 4 together with the corresponding broadening energy $\hbar/\tau_3^{ee}$ according to Eq. (7). For comparison, we also present the quadratic temperature dependence of the broadening energy in the lower subbands, $\hbar/\tau^{ee} = \lambda T^2/\varepsilon_F$ [see Eq. (1)], caused by electron-electron scattering. The constant $\lambda = 2.2$ in this expression is
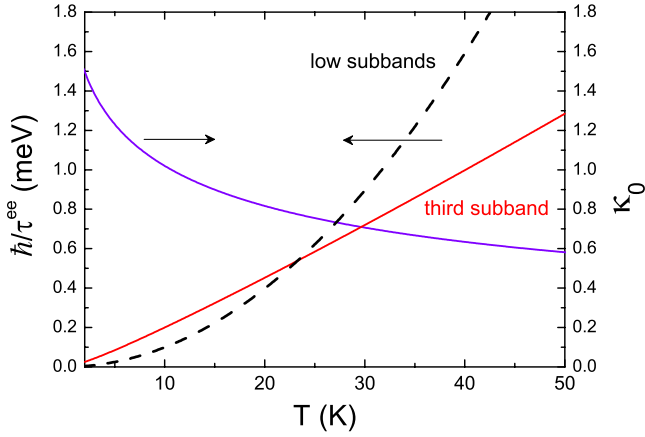
FIG. 4. (Color online) Function $\kappa_0(T)$ for our WQW system and temperature dependence of the inverse quantum lifetime of electrons in the third subband due to electron-electron scattering. The dashed line corresponds to the inverse quantum lifetime of electrons in the first and second subbands, according to Eq. (1).

determined from experimental data on thermal suppression of the large-period MIS oscillations in our samples.

Figure 4 demonstrates that temperature dependence of the quantum lifetime of electrons in the third subband is weaker than in the first and second subbands. The reason for this behavior is rooted in the fact that the third subband is almost empty and contains nondegenerate electron gas (see Appendix for details).

As the self-energy is defined, calculation of the density of states in the subband 3 is done according to Eq. (6) by taking the sum over Landau levels n numerically. The result of the calculations for $B=0.4$ T and two chosen temperatures is demonstrated in Fig. 5 and represents a physically reasonable picture when temperature-dependent energy $\hbar/\tau_3^{ee}$ describes broadening of both the Landau levels and subband edge. In spite of the profound quantization, the Landau levels are still overlapping, and the oscillating density of states at 20 K can
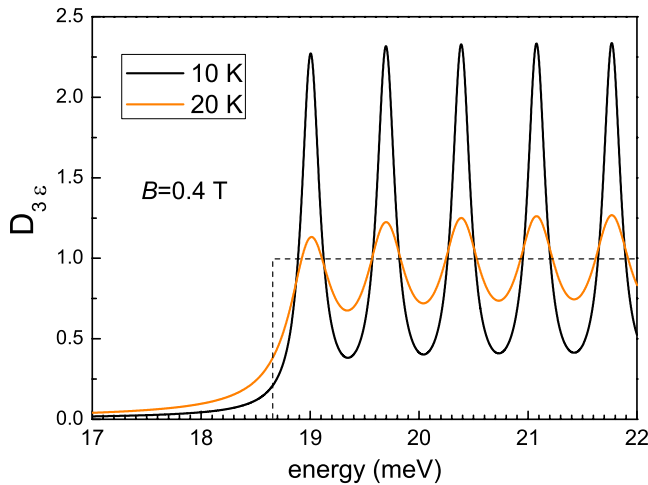

FIG. 5. (Color online) Examples of the density of electron states in the third subband of our WQW system. The dashed line shows an "ideal" 2D density of states in the absence of the magnetic field and collision-induced broadening.

be approximated, with a good accuracy, by a harmonic oscillation function.

Next, calculations of the density of states in the two lowest subbands are carried out within the self-consistent Born approximation, using the quantum lifetime described by Eq. (1) with elastic-scattering contribution $\tau(0)=6.6$ ps determined from low-temperature magnetoresistance. Substituting the calculated D_ε and $D_{3\varepsilon}$ into Eq. (5), we finally describe the resistivity. Apart from this numerical calculation, it is useful to present an analytical result

$$\rho_d = \frac{m\nu_{tr}}{e^2 n_s}\left[1 + \eta f_{\varepsilon_3} + d^2\left(1 + \cos\frac{2\pi\Delta_{12}}{\hbar\omega_c}\right)\right.$$
$$\left. + \eta f_{\varepsilon_3} d d_3\left(\cos\frac{2\pi\Delta_{13}}{\hbar\omega_c} + \cos\frac{2\pi\Delta_{23}}{\hbar\omega_c}\right)\right], \quad (8)$$

based on the approximate (single-harmonic) representation of the densities of states: $D_\varepsilon \simeq 1 - d(\cos[2\pi(\varepsilon-\varepsilon_1)/\hbar\omega] + \cos[2\pi(\varepsilon-\varepsilon_2)/\hbar\omega])$ and $D_{3\varepsilon} \simeq 1 - 2d_3 \cos[2\pi(\varepsilon-\varepsilon_3)/\hbar\omega]$ at $\varepsilon > \varepsilon_3$. The Dingle factor d is given by Eq. (1) while the Dingle factor for the third subband is $d_3 = \exp[-\pi/\omega_c\tau_3^{ee}(T)]$. Equation (8) is valid when T exceeds the broadening energy $\hbar/\tau_3^{ee}$ and when $2\pi^2 T \gg \hbar\omega_c$, so the SdH oscillations are thermally averaged out. The terms associated with the third subband in Eq. (8) describe small-period oscillations due to large subband separation energies Δ_{13} and Δ_{23}. The amplitude of these oscillations is governed, apart from the product of the Dingle factors dd_3, by a small factor ηf_{ε_3}. The same factor determines a correction to the background (nonoscillating) resistivity. The relative contribution of this correction at $T < 30$ K does not exceed 6% and does not lead to an appreciable increase in the resistivity with temperature. The increase in the background resistivity observed in experiment, see Fig. 2, is described by thermal enhancement of electron scattering by acoustic phonons.

The comparison of the measured and calculated resistivity at two chosen temperatures, 10 and 15 K, is shown in Fig. 6. First of all, by comparing the periodicity of small-period oscillations we determine the position of the third subband and find that it is placed at 2.2 meV above the Fermi energy (in other words, $\Delta_{13}=19.36$ meV and $\Delta_{23}=17.96$ meV). Below 0.6 T the theoretical and experimental plots show a good agreement while in the region of the first MIS peak ($B \sim 0.8$ T) the experiment shows a considerably smaller magnetoresistance than it is expected from the theory. This deviation occurs only in the temperature range we have studied in the present work and is absent at low temperatures ($T < 4.2$ K). We do not know exactly the reason for this deviation, probably it is associated with some mechanisms of Landau-level broadening not taken into account or with the influence of electron-phonon scattering on magnetotransport.[28] As concerns the small-period MIS oscillations, the best fit of their amplitudes to experimental values is obtained in the whole region of magnetic fields by considering η as a single adjustable parameter of our theory, set at a reasonable value $\eta=0.2$ (a calculation of η is possible in general, but requires a detailed knowledge of impurity nature and distribution). Notice that the results of numerical and analytical methods of calculations are in a reasonable accor-
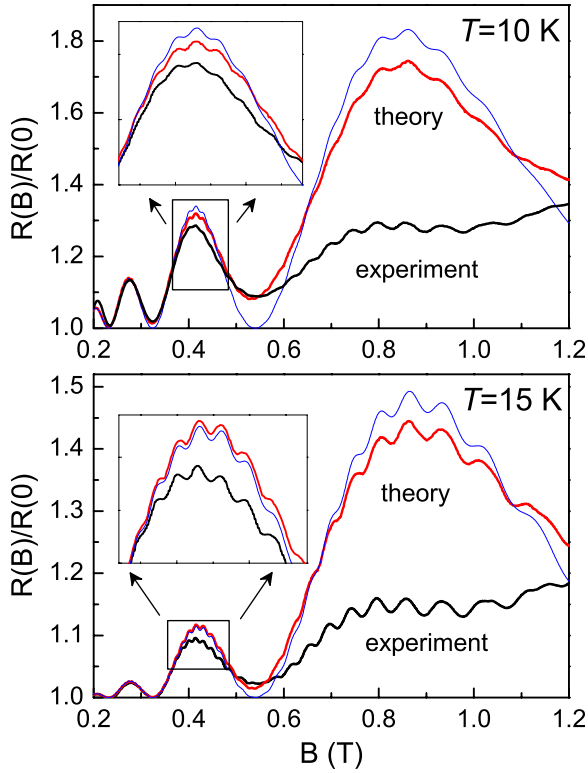
FIG. 6. (Color online) Measured and calculated magnetoresistance for our WQW system. Two kinds of theoretical plots are shown: based on a numerical calculation (thick line, red) and on analytical expression (8) (narrow line, blue). The regions around 0.4 T are blown up.

dance, which indicates the reliability of the analytical approach of Eq. (8) and validity of the conditions of overlapping Landau levels. Similar calculations at the other temperatures also demonstrate a good agreement.

We also applied the results of our calculations for description of the temperature dependence of MIS oscillations of both kinds. As found experimentally, the small-period MIS oscillations experience a thermal-activated behavior at low temperatures and a weaker (compared to large-period MIS oscillation) thermal suppression at larger temperatures. Although both these features are now qualitatively understood, it is instructive to compare directly the experimental data on peak-to-peak amplitudes shown in Fig. 3 with corresponding theoretical results following from the analytical expression (8). Such theoretical plots are added to Fig. 3 and show a good agreement with experiment concerning both nonmonotonic temperature dependence of the small-period MIS oscillation amplitudes in the region of $T = 8-15$ K and the decrease in these amplitudes at elevated temperatures.

IV. CONCLUSIONS

We have designed a WQW structure with high electron density, where two lowest closely spaced subbands are occupied by electrons while the third subband is placed slightly above the Fermi energy and, therefore, is not occupied at low temperatures (Fig. 1). By measuring the magnetoresistance

of this system, we have detected thermally activated MIS oscillations caused by elastic scattering of electrons between the third subband and the two lower subbands. These small-period MIS oscillations demonstrate an unusually slow suppression at higher temperatures as compared to the well-established temperature dependence of the large-period MIS oscillations caused by electron scattering between the lowest (occupied) subbands. Our theoretical study has uncovered the reasons for this behavior. The temperature dependence for both kinds of MIS oscillations is determined by the influence of electron-electron scattering on the Landau-level broadening. However, the widely accepted T^2 scaling of the broadening energy cannot be applied to the case of an almost empty subband, where the carriers have kinetic energies on the order of T and form a nondegenerate electron gas near the subband bottom. For such a case, a detailed calculation shows that the broadening energy scales with temperature slower than $T^{3/2}$, depending on the shape of the wave functions determined by the confinement potential. The theoretical dependence of the resistivity on the magnetic field and temperature explains all essential details of our experimental results.

To the best of our knowledge, thermally activated MIS oscillations have not been reported previously in magnetoresistance measurements. In our research, based on a particular structure design, we have demonstrated that the existence of such oscillations opens different ways in applications of magnetotransport experiments to study electron energy spectrum and scattering mechanisms in multisubband systems. We assume that this research will stimulate further experimental and theoretical studies in this direction.

APPENDIX: QUANTUM LIFETIME OF ELECTRONS IN THE UPPER SUBBAND

We start our consideration of electron-electron scattering by neglecting the processes in which electrons are transferred between subbands because such processes require large transferred momenta $\hbar\mathbf{q}$ and, for this reason, are strongly suppressed, especially in wide quantum wells. The remaining processes can be viewed as scattering of electrons in the subband j by electrons resting either in the same subband or in the other subbands. The imaginary part of the self-energy due to electron-electron scattering is written, in the momentum representation, as

$$\mathrm{Im}\,\Sigma^{(ee)A}_{\varepsilon j \mathbf{p}} = 2\pi \sum_{j'} \int \frac{d\mathbf{p}'}{(2\pi\hbar)^2} \int \frac{d\mathbf{q}}{(2\pi)^2} U^2_{jj'}(q)$$

$$\times \int d\varepsilon' \int dE\, \delta(\varepsilon + E - \varepsilon_{j\mathbf{p}+\hbar\mathbf{q}})\,\delta(\varepsilon' - E$$

$$- \varepsilon_{j'\mathbf{p}'-\hbar\mathbf{q}})\,\delta(\varepsilon' - \varepsilon_{j'\mathbf{p}'})[f_{\varepsilon'}(1 - f_{\varepsilon+E} - f_{\varepsilon'-E})$$

$$+ f_{\varepsilon+E}f_{\varepsilon'-E}], \tag{A1}$$

where $\varepsilon_{j\mathbf{p}}=\varepsilon_j+p^2/2m$, E is the energy transferred in collisions, and $U_{jj'}(q)$ is the effective interaction potential

$$U_{jj'}(q) = \frac{2\pi e^2}{\epsilon(q+q_0)}I_{jj'}(q),$$

$$I_{jj'}(q) = \int dz \int dz' e^{-q|z-z'|}|\psi_{jz}|^2|\psi_{j'z'}|^2. \quad \text{(A2)}$$

Here ϵ is the dielectric constant, $q_0=2e^2m/\hbar^2\epsilon$ is the inverse screening length, and ψ_{jz} is the envelope wave function for subband j. The overlap factor $I_{jj'}(q)$ is often set to unity in description of the scattering with small transferred momentum which is essential at $T \ll \varepsilon_F$. However, in wide quantum wells (like those used in our experiment) this factor becomes important and leads to a significant (2–3 times) suppression of the Coulomb interaction, so we keep it in our consideration. To find $I_{jj'}(q)$, we use the eigenstates ψ_{jz} obtained in the self-consistent calculation of the energy spectrum of our WQW (Fig. 1). Equation (A1) can be derived, for example, from the expressions for Green's functions and self-energies presented in Ref. 29; a generalization of these expressions for multisubband systems is straightforward. Notice that the Green's functions of electrons in this derivation are taken in the free-particle approximation, which leads to the appearance of the δ functions of energies in Eq. (A1).

The processes contributing to the self-energy of the third subband, $\Sigma_{\varepsilon3\mathbf{p}}^{(ee)A}$, include scattering between electrons in the same (third) subband, $j'=j=3$, as well as the scattering between electrons in the third and in the lower subbands, $j'=1,2$. Since the occupation of the third subband by electrons is low and $f_{\varepsilon_3} \ll 1$ corresponds to the case of nondegenerate electron gas, the latter processes are more significant and are considered in the following. For this kind of scattering, the integrals over the variables ε', $\mathbf{p}'$, and over the angle of the vector $\mathbf{q}$ in Eq. (A1) can be calculated analytically. Further, expressing the quantum lifetime for the third subband according to $1/\tau_{3\varepsilon}^{ee}=(2/\hbar)\text{Im}\,\Sigma_{\varepsilon3\mathbf{p}}^{(ee)A}|_{\varepsilon_{3\mathbf{p}}=\varepsilon}$, we get

$$\frac{\hbar}{\tau_{3\varepsilon}^{ee}} = \sum_{j=1,2} \frac{1}{\pi v_{Fj}\sqrt{2m}} \int_{-(\varepsilon-\varepsilon_3)}^{\infty} dE \int_{\varepsilon_q^{(-)}}^{\varepsilon_q^{(+)}} d\varepsilon_q$$
$$\times \frac{E}{\sqrt{\varepsilon_q[4\varepsilon_q(\varepsilon-\varepsilon_3)-(E-\varepsilon_q)^2]}} \frac{I_{3j}^2(q)}{(1+q/q_0)^2}$$
$$\times \left[f_{\varepsilon+E} + \frac{1}{e^{E/T}-1}\right], \quad \text{(A3)}$$

where v_{Fj} is the Fermi momentum for one of the lower subbands, $\varepsilon_q=\hbar^2q^2/2m$, $\varepsilon_q^{(\pm)}=(\sqrt{\varepsilon-\varepsilon_3+E}\pm\sqrt{\varepsilon-\varepsilon_3})^2$ Under conditions of our experiment, the difference between v_{F1} and v_{F2} is not essential, so $v_{F1}=v_{F2}=\sqrt{2\varepsilon_F/m}$, where $\varepsilon_F=\hbar^2\pi n_s/2m$. Next, since $f_{\varepsilon_3} \ll 1$, the term proportional to $f_{\varepsilon+E}$ can be neglected in Eq. (A3). As a result, the quantum lifetime is represented as

$$\frac{\hbar}{\tau_{3\varepsilon}^{ee}} = \kappa_{\varepsilon-\varepsilon_3}(T)\frac{T^{3/2}}{\sqrt{\varepsilon_F}}, \quad \text{(A4)}$$

where κ is a dimensionless function of energy and temperature. Numerical calculation of κ shows that its energy dependence near the edge of the third subband ($\varepsilon_3<\varepsilon<\varepsilon_3+T$) appears to be weak in the important temperature interval from 10 to 30 K. Therefore, below we treat the quantum lifetime as energy-independent quantity by taking κ at the edge of the third subband, $\kappa_{\varepsilon-\varepsilon_3}(T)\simeq\kappa_0(T)$. Then we obtain the expression

$$\kappa_0(T) = \int_0^{\infty} dx\frac{\sqrt{x}}{e^x-1}F_T(x),$$

$$F_T(x) = \frac{I_{31}^2(q_x)+I_{32}^2(q_x)}{2(1+q_x/q_0)^2}, \quad q_x = \frac{\sqrt{2mTx}}{\hbar}, \quad \text{(A5)}$$

where we introduced a dimensionless variable $x=E/T$. Temperature dependence of $\kappa_0(T)$ takes place mostly because of the sensitivity of the squared overlap factors I_{31}^2 and I_{32}^2 to transferred energy E (which, near the edge of the third subband, is directly connected to the transferred momentum, $E\simeq\varepsilon_q$). This sensitivity is caused by the large width of our quantum well and is essentially determined by the form of the wave functions ψ_{jz} shown in Fig. 1. The function $\kappa_0(T)$ calculated according to Eq. (A5) is presented in Fig. 4.

In narrow wells, where the characteristic wave number q is small in comparison to the inverse well width, the suppression factor $F_T(x)$ in Eq. (A5) can be approximated by unity, leading to the universal result $\kappa_0(T)\simeq2.3$. Then we obtain the dependence $1/\tau_3^{ee}\propto T^{3/2}$ which is weaker than $1/\tau^{ee}\propto T^2$ characterizing temperature dependence of quantum lifetime in the lower subbands [Eq. (1)]. In wide wells, where the wave number q, limited by temperature, may exceed the inverse well width, an additional weakening takes place, so the temperature dependence of $1/\tau_3^{ee}$ calculated for our system and shown in Fig. 4 is different from $T^{3/2}$ and roughly resembles a linear function.

[1] D. Shoenberg, *Magnetic Oscillations in Metals* (Cambridge University Press, Cambridge, 1984).

[2] V. Polyanovsky, Fiz. Tekh. Poluprovodn. **22**, 2230 (1988) [Sov. Phys. Semicond. **22**, 1408 (1988)].

[3] P. T. Coleridge, Semicond. Sci. Technol. **5**, 961 (1990).

[4] D. R. Leadley, R. Fletcher, R. J. Nicholas, F. Tao, C. T. Foxon, and J. J. Harris, Phys. Rev. B **46**, 12439 (1992).

[5] T. H. Sander, S. N. Holmes, J. J. Harris, D. K. Maude, and J. C. Portal, Phys. Rev. B **58**, 13856 (1998).

[6] N. C. Mamani, G. M. Gusev, T. E. Lamas, A. K. Bakarov, and O. E. Raichev, Phys. Rev. B **77**, 205327 (2008).

[7] A. A. Bykov, D. P. Islamov, A. V. Goran, and A. I. Toropov, JETP Lett. **87**, 477 (2008).

[8] A. V. Goran, A. A. Bykov, A. I. Toropov, and S. A. Vitkalov,

Phys. Rev. B **80**, 193305 (2009).

[9] A. A. Bykov, A. V. Goran, and S. A. Vitkalov, Phys. Rev. B **81**, 155322 (2010).

[10] S. Wiedmann, N. C. Mamani, G. M. Gusev, O. E. Raichev, A. K. Bakarov, and J. C. Portal, Phys. Rev. B **80**, 245306 (2009).

[11] D. Konstantinov and K. Kono, Phys. Rev. Lett. **103**, 266808 (2009).

[12] N. S. Averkiev, L. E. Golub, S. A. Tarasenko, and M. Willander, J. Phys.: Condens. Matter **13**, 2517 (2001).

[13] K.-J. Friedland, R. Hey, H. Kostial, R. Klann, and K. Ploog, Phys. Rev. Lett. **77**, 4616 (1996).

[14] A. T. Hatke, M. A. Zudov, L. N. Pfeiffer, and K. W. West, Phys. Rev. Lett. **102**, 066804 (2009).

[15] I. A. Dmitriev, M. G. Vavilov, I. L. Aleiner, A. D. Mirlin, and D. G. Polyakov, Phys. Rev. B **71**, 115316 (2005).

[16] I. A. Dmitriev, M. Khodas, A. D. Mirlin, D. G. Polyakov, and M. G. Vavilov, Phys. Rev. B **80**, 165327 (2009).

[17] G. W. Martin, D. L. Maslov, and M. Yu. Reizer, Phys. Rev. B **68**, 241309(R) (2003).

[18] S. Engelsberg and G. Simpson, Phys. Rev. B **2**, 1657 (1970).

[19] Y. Adamov, I. V. Gornyi, and A. D. Mirlin, Phys. Rev. B **73**, 045426 (2006).

[20] I. B. Berkutov, V. V. Andrievskii, Yu. F. Komnik, O. A. Mironov, M. Mironov, and D. R. Leadley, Low Temp. Phys. **35**, 141 (2009).

[21] S. Syed, M. J. Manfra, Y. J. Wang, R. J. Molnar, and H. L. Stormer, Appl. Phys. Lett. **84**, 1507 (2004).

[22] M. G. Vavilov and I. L. Aleiner, Phys. Rev. B **69**, 035303 (2004).

[23] I. A. Dmitriev, F. Evers, I. V. Gornyi, A. D. Mirlin, D. G. Polyakov, and P. Wolfle, Phys. Status Solidi B **245**, 239 (2008).

[24] O. E. Raichev, Phys. Rev. B **78**, 125304 (2008).

[25] O. E. Raichev, Phys. Rev. B **81**, 195301 (2010).

[26] N. C. Mamani, G. M. Gusev, E. C. F. da Silva, O. E. Raichev, A. A. Quivy, and A. K. Bakarov, Phys. Rev. B **80**, 085304 (2009).

[27] N. C. Mamani, G. M. Gusev, O. E. Raichev, T. E. Lamas, and A. K. Bakarov, Phys. Rev. B **80**, 075308 (2009).

[28] Both theory and experiment show a considerable reduction in the phonon-assisted part of the resistivity in the region of magnetic fields $\omega_c > 2k_F s_l$, where k_F is the Fermi wave number ($k_F \simeq \sqrt{\pi n_s}$ for our two-subband system) and s_l is the acoustic phonon velocity: see, e.g., O. E. Raichev, Phys. Rev. B **80**, 075318 (2009), and references therein. Although the first MIS peak in our experiment appears in this region of fields, the magnitude of the effect, according to our estimates, is still weak for satisfactory explanation of the deviation.

[29] O. E. Raichev, Phys. Rev. B **81**, 165319 (2010).